

CHEMISTRY

A European Journal



Accepted Article

Title: Dispirocycles: Novel Platforms for Construction of High-Performance Host Materials for Phosphorescent Organic Light-Emitting Diodes

Authors: Jian Fan, Xiang-Yang Liu, Yi-Jie Zhang, Xiyu Fei, and Man-Keung Fung

This manuscript has been accepted after peer review and appears as an Accepted Article online prior to editing, proofing, and formal publication of the final Version of Record (VoR). This work is currently citable by using the Digital Object Identifier (DOI) given below. The VoR will be published online in Early View as soon as possible and may be different to this Accepted Article as a result of editing. Readers should obtain the VoR from the journal website shown below when it is published to ensure accuracy of information. The authors are responsible for the content of this Accepted Article.

To be cited as: *Chem. Eur. J.* 10.1002/chem.201806207

Link to VoR: <http://dx.doi.org/10.1002/chem.201806207>

Supported by
ACES

WILEY-VCH

DOI: 10.1002/((please add manuscript number))

Article type: Full Paper

Dispirocycles: Novel Platforms for Construction of High-Performance Host Materials for Phosphorescent Organic Light-Emitting Diodes

Xiang-Yang Liu, † Yi-Jie Zhang, † Xiyu Fei, Man-Keung Fung, and Jian Fan**

Jiangsu Key Laboratory for Carbon-Based Functional Materials & Devices, Joint International Research Laboratory of Carbon-Based Functional Materials and Devices, Institute of Functional Nano & Soft Materials (FUNSOM), Soochow University, Suzhou, Jiangsu 215123, China

† The two authors contribute equally to this paper.

E-mail: mkfung@suda.edu.cn (Prof. M.-K. Fung); jianfan@suda.edu.cn (Prof. J. Fan).

Keywords: (Dispirocycles, Host materials, Phosphorescence, OLEDs, Triplet energy)

Abstract: Spirocycle compounds such as 9,9'-Spirobifluorene (SBF) are becoming more and more attractive for use as the host materials in organic optoelectronic devices. In this manuscript, two dispirocycles, namely dispiro[fluorene-9,9'-anthracene-10',9''-fluorene] and 10,10''-diphenyl-10*H*,10''*H*-dispiro[acridine-9,9'-anthracene-10',9''-acridine] were used for the construction of hosts materials (**1**, **2**, **3**, and **4**). The attached triphenylamine group would determine the thermal, photophysical, electrochemical, and charge transport properties, and therefore they have different electroluminescence performances. The device based on dispiro[fluorene-9,9'-anthracene-10',9''-fluorene] (**2**) and 10,10''-diphenyl-10*H*,10''*H*-dispiro[acridine-9,9'-anthracene-10',9''-acridine] (**3**) molecular platforms exhibited a external quantum efficiency of over 21% with a very high power efficiency (~100 lm W⁻¹). The results here demonstrate to us the potential of extending the possibilities of applying the dispirocyclic molecular platforms with inherent rigidity for developing highly efficient host materials for OLEDs.

Since 9,9'-Spirobifluorene (SBF) was first reported in 1930,^[1] it has attracted considerable attention and has been successfully applied in various fields^[2-12] such as asymmetric catalysts,^[2] macrocyclic sensors,^[3] self-assembling structures,^[4] porous materials,^[5] and organic electronics.^[6-12] It is well known that there are four isomeric mono-substituted SBF derivatives (Figure 1), and their synthesis methods are well established.^[13-16] So far the most common di-substituted SBF derivatives are the compounds with substituents at the 2,7-positions or 3,6-positions. From a chemist's point of view, the symmetrically 2,7-^[17] or 3,6-^[18] substituted SBF and asymmetrically 2,2'-, or 3,3'-substituted SBF^[19] can be readily prepared relative to other di-substituted SBF derivatives. For the tetra-substituted compounds, the 2,2',7,7'-tetrasubstituted SBF are positioned along two perpendicular axes while 3,3',6,6'-tetrasubstituted SBF reveals a tetrahedral orientation. When the two substituents (R1 and R2) are located on different fluorene motifs, the di-substituted SBF molecular are chiral (axial chirality) and it does not matter whether $R1 = R2$ or $R1 \neq R2$.^[20,21] Compared to 2,7-^[17] or 3,6-^[18] substituted SBF, the straightforward and efficient synthesis methods of 1,8- and 4,5-disubstituted SBF derivatives are still highly desirable.^[22,23] So far, a plethora of synthetic methods have been developed for the functionalization of SBF.^[15a,24] From a synthetic point of view, the functionalization of SBF can be accomplished after the SBF core is available or with decoration of the fluorene motif and the related precursors at an early stage.^[25-28] For example, the symmetric 2,2',7,7'-substituted SBF can be prepared with tetra-halogenated (bromide or iodide) SBF precursors.^[21,25,26]

Recently, SBF derivatives are gaining increasing interest in the research area of organic electronics,^[14-16,29] and many novel spirocycles with various levels of structural diversity have been developed in the pursuit of high performance of electronic devices. In addition, modern synthetic methodology allows the molecular fragments and functional groups to be manipulated in many innovative ways which promotes the discovery of novel materials. Much research effort has concentrated on the development of highly efficient OLEDs materials,^[30-35] and a variety of SBF analogues (Figure 2) have been used as novel molecular platforms. In particular, several dispiro-compounds have been reported and applied to efficient OLEDs (Figure 3).^[36-40] For instance, Poriel, *et al.*, reported a series of dispirofluorene-indenofluorene (DSF-IF) isomers, which were used as high efficiency OLEDs materials.^[36] So far, the application of dispiro[fluorene-9,9'-anthracene-10',9''-fluorene] (DSFA) and dispiro[acridine-9,9'-anthracene-10',9''-acridine] (DSAA) derivatives as host material has been rarely reported. Herein, we designed and synthesized four novel dispirocyclic compounds, 2'-(*tert*-butyl)dispiro[fluorene-9,9'-anthracene-10',9''-fluorene] (**1**), 4-(dispiro[fluorene-9,9'-

WILEY-VCH

anthracene-10',9''-fluoren]-2'-yl)-*N,N*-diphenylaniline (**2**), 4-(10,10''-diphenyl-10*H*,10''*H*-dispiro[acridine-9,9'-anthracene-10',9''-acridin]-2'-yl)-*N,N*-diphenylaniline (**3**), and 2'-(*tert*-butyl)-10,10''-diphenyl-10*H*,10''*H*-dispiro[acridine-9,9'-anthracene-10',9''-acridine] (**4**). The thermal stabilities, photophysical properties, and electrochemical behaviors of these four compounds were investigated systematically. The electron-donating group, triphenylamine, was introduced to tune the charge transport capability. The device performance of these compounds was studied as host material. The OLED devices hosted by **2** and **3** with bis(2-phenylpyridine) (acetylacetonate)iridium (III) (Ir(ppy)₂(acac)) as a green dopant exhibited a device performance with a maximum external quantum efficiency of over 21%. It is worth noting that the power efficiencies of **2**- and **3**-based devices reached about 100 lm W⁻¹, which would encourage us to pursue a further investigation based on dispiro compounds.

The synthetic routes of **1**, **2**, **3**, and **4** as illustrated in Scheme 1. 2-(*tert*-butyl)anthracene-9,10-dione and 2-bromoanthracene-9,10-dione were treated with 2-lithiumbiphenyl or (2-(diphenylamino)phenyl)lithium to obtain the corresponding tertiary alcohols, and the acid catalyzed cyclization reaction yields **1**, **2a**, **3a**, and **4**.^[38a,41] The products of **2** and **3** can be obtained through the Suzuki–Miyaura C–C coupling reaction between the respective dispiro compounds **2a** and **3a** and (4-(diphenylamino)phenyl)boronic acid with good yields. The structures of the target products were fully characterized by ¹H/¹³C NMR spectroscopy, mass spectrometry (MS) and elemental analysis (EA).

As shown in Figure 4 and Figure 5, the thermal properties of **1**, **2**, **3**, and **4** were examined via differential scanning calorimetry (DSC) and thermogravimetric analysis (TGA) under a nitrogen atmosphere. The corresponding glass transition temperatures (*T_g*)/ crystallization temperatures (*T_c*)/ melting point (*T_m*)/ decomposition temperatures (*T_d*, 5 wt% weight loss) of **1**, **2**, **3**, and **4** were -/-/351/334 °C, -/-/333/438 °C, 132/230/-/490 °C, and 134/-/392/396 °C, respectively (Table 1). It is worth noting that the *T_g* values of **1** and **2** were not observed. On the other hand, the nearly 100% weight loss of **1**, **2**, and **4** at above 400 °C could be due to sublimation, which suggests that these spirans are stabilized at those temperatures and can be thermally deposited for device fabrication.

Room temperature ultraviolet-visible (UV-Vis) absorption and photoluminescence (PL) spectra and low temperature (77 K) phosphorescence (Phos) spectra of **1**, **2**, **3**, and **4** were measured in toluene. As shown in Figure 6, **1** and **2** give well-defined absorption peaks at around 300/311

nm and 300/311/337 nm, respectively. In contrast, **3** and **4** show broad and structureless absorption and maximum absorption peaks at around 323 nm and 310 nm, respectively, which might be due to the relatively flexible structures of **3** and **4**. Moreover, the absorption band in the range of 320-370 nm for compound **2** could arise from the triphenylamine segment. The absorption onsets of **1**, **2**, **3**, and **4** are 316 nm, 370 nm, 370 nm, and 340 nm, respectively. Therefore, the corresponding optical energy gaps (E_{gs}) of **1**, **2**, **3**, and **4** were estimated to be 3.92 eV, 3.35 eV, 3.35 eV, and 3.63 eV, respectively. The introduction of the triphenylamine unit led to a conspicuous red-shift in **2** and **3** in comparison with **1** and **4**. As shown by the PL curves, compound **1** exhibited well-defined emission with peaks at 316 nm and 327 nm, and **2-4** compounds showed structureless spectra with peaks at 385 nm, 385 nm, and 348 nm, respectively. For compounds **1**, **4** and **3**, their PL emission peaks are red-shifted gradually with the increase in the number of electron-donating group triphenylamine. All these compounds exhibited well-defined Phos emission curves and the corresponding triplet energies (E_{Ts}) can be calculated by the highest vibronic band of **1** (434 nm), **2** (482 nm), **3** (481 nm), and **4** (408 nm), which are 2.86 eV, 2.57 eV, 2.58 eV, and 3.04 eV, respectively. So these four compounds can be used as host material for green PHOLEDs.

It is worth noting that **2** and **3** show nearly identical PL spectra and quite similar Phos spectra, so they have similar lowest singlet (S_1) and triplet (T_1) excited states. In order to gain more insights into the excited state characteristics of **1**, **2**, **3**, and **4**, natural transition orbitals (NTOs) were used to describe their S_1 and T_1 excitations.^[42] The NTO (hole and particle) distributions and the weight of hole-particle contribution to S_1 and T_1 are shown in Figure 7. The holes of S_1 of **1** are mainly distributed on the fluorene unit and one phenyl group of 9,10-dihydroanthracene fragment. The corresponding particles, however, are primarily limited to the fluorene unit. In compound **4**, the holes and particles of S_1 are mainly localized on the 9,10-dihydroacridine and *N*-phenyl group, respectively. It is worth noting that the holes and particles of the S_1 states of **2** and **3** have essentially the same distributions, namely, the holes are mainly localized on the diphenylamine units and the particles are primarily dispersed along the biphenyl segments (one phenyl group comes from triphenylamine and the other from 9,10-dihydroanthracene). Considering the similar molecular structures and similar S_1 characteristics observed in **2** and **3**, it is not surprising that these two compounds have essentially identical PL spectra. In addition, the S_1 states of compound **1** feature a local excitation (LE) character and the S_1 states of the other three compounds exhibit a charge-transfer (CT) excitation character, which agrees well with the shape of their PL curves. The distributions of holes and particles of T_1 in **1** and **4** are

confined to the fluorene and 9,10-dihydroacridine segments, respectively. On the other hand, the distributions of T_1 holes and particles in **2** and **3** are mainly confined to the biphenyl fragment, which could explain their similar E_T values. As a result, the holes and particles of T_1 of **1-4** are mainly located on the same fragment in each compound, indicating the LE character, which is consistent with their well-defined Phos emissions.

The electrochemical behaviors of **1**, **2**, **3**, and **4** were further investigated by cyclic voltammetry (CV) measurement in dichloromethane solution. The cyclic voltammograms are shown in Figure 8 and the detailed results are summarized in Table 1. **1**, **2**, **3**, and **4** show the oxidation processes during the anodic scan, and the corresponding onsets of the first oxidation waves were 1.44 V, 0.85 V, 0.86 V, and 0.96 V. Therefore, the highest occupied molecular orbitals (HOMO) energy levels are estimated to be -5.82 eV, -5.23 eV, -5.24 eV, and -5.34 eV, respectively. On the other hand, the lowest unoccupied molecular orbitals (LUMO) energy levels of **1**, **2**, **3**, and **4** can be calculated by their E_g s and the corresponding HOMO energy levels, which are -1.90 eV, -1.80 eV, -1.89 eV, and -1.71 eV, respectively. Furthermore, to better understand the relationship between molecular structure and electronic structure, density function theory (DFT) calculations are carried out to simulate the HOMO/LUMO distributions and energy levels and the optimized geometry of **1**, **2**, **3**, and **4** at a B3LYP/6-31G(d) level (Figure 9). As shown in Figure 9, the HOMO distributions of **1**, **2**, **3**, and **4** are quite different. Since there is no strong electron-donating group in **1**, the HOMO of compound **1** is distributed over the whole molecule. For **2** and **3**, the HOMOs are localized at the triphenylamine segments and extended partially over one phenyl group of the 9,10-dihydroanthracene unit. As for compound **4**, the HOMO is mainly distributed on the 9,10-dihydroacridine unit. It is worth noting that compounds **2** and **3** have similar HOMO energy levels due to their similar HOMO contribution unit. Meanwhile, the LUMO distributions of **1**, **2**, **3**, and **4** are also quite different. The LUMOs are mainly localized in the fluorene parts for **1** and **2**, and two phenyl groups (one from triphenylamine and the other from 9,10-dihydroanthracene) for **3**. However, the LUMO of **4** are spread over the whole backbone. So the similar LUMO distributions of **1** and **2** led to a small difference in their LUMO energy levels. The introduction of the electron-donating triphenylamine group into the skeletons of **2**, **3** and **4** results in their shallow HOMO energy levels. These results match well with the experimental (CV) data.

To study the capability of these four dispirocycles (**1**, **2**, **3**, and **4**) as host material in PHOLEDs, green devices were fabricated with Ir(ppy)₂(acac) as dopant. The device structure is described

as follows: ITO/ HAT-CN (10 nm)/ TAPC (55 nm)/ Host: 10 wt% Ir(ppy)₂(acac) (20 nm)/ B4PyMPM (40 nm)/ Liq (2 nm)/ Al (120 nm). The current density–voltage–luminance (J – V – L) characteristics, current efficiency (CE)/power efficiency (PE)/external quantum efficiency (EQE) versus L plots, and electroluminescent (EL) spectra as depicted in Figure 10, and the detailed parameters are summarized in Table 2.

As shown by the J – V – L characteristics curves (Figure 10(a)), all four devices exhibited relatively low driving voltages at a luminance of 200 cd m⁻² with 3.24 V for **1**, 2.47 V for **2**, 2.53 V for **3** and 2.65 V for **4**, indicating that the introduction of the electron-donating triphenylamine group can improve the hole transport properties of the host materials, no matter whether a triphenylamine motif was involved in the backbone (**3** and **4**) or acting as a side chain (**2**). Furthermore, the hole- and electron-transport performance of these materials was further studied with hole-only and electron-only devices: ITO/MoO₃ (10 nm)/**1**, **2**, **3**, or **4** (100 nm)/MoO₃ (10 nm)/Al (100 nm) (hole-only devices) and ITO/TmPyPB (20 nm)/**1**, **2**, **3**, or **4** (100 nm)/TmPyPB (20 nm)/Liq (2 nm)/Al (100 nm) (electron-only devices). The J – V characteristics of single carrier devices are presented in Figure 11. As expected, **1**, **2**, **3**, and **4** are typical unipolar materials, their hole transport abilities are significantly better than their corresponding electron transport abilities. In addition, **2**, **3**, and **4** demonstrate similar hole-/electron-transport properties, but superior to **1**, which could account in part for the trend of their device driving voltages.

Figure 10(b) gives the device efficiencies based on **1**–**4**, labeled as G1–G4. All of the devices displayed a satisfactory device performance. The device based on **2** (G2) achieved the highest device performance among G1–G4 with a maximum CE and EQE of 78.0 cd A⁻¹ and 21.7%, respectively. On the other hand, the device using **3** as the host material (G3) also obtained a high device efficiency with a maximum CE of 76.0 cd A⁻¹ and EQE of 21.3%. It is worth noting that the PEs of G2 and G3 are as high as 100.5 lm W⁻¹ and 96.1 lm W⁻¹, respectively, which are comparable to the state-of-the-art results based on Ir(ppy)₂(acac).^[43] The maximum CE, PE, and EQE of device G4 (hosted by **4**) are 65.0 cd A⁻¹, 80.0 lm W⁻¹, and 18.3%, respectively. However, the device performance of G1 (hosted by **1**) is relatively lower than that of G2–G4, and the maximum CE, PE and EQE are 57.0 cd A⁻¹, 59.5 lm W⁻¹, and 16.0%, respectively. The remarkable performance of G2 might be attributed to its high E_T and good charge transport capacity.^[44] The high E_T could favor the energy transfer process from the host to the dopant and block the energy transfer process from the dopant back to the host since no other emission was observed from the EL spectra. On the other hand, the good charge transport ability may decrease the driving voltage and lead to a high PE value. The EL spectra of devices G1–G4 are shown in

Figure 10(c). All of the devices exhibit a typical Ir(ppy)₂(acac) emission with a peak at 520 nm, which means the triplet excitons are confined efficiently in the dopant. The CIE coordinates of G1-G4 at a current density of 5 mA cm⁻² are (0.33, 0.63), (0.34, 0.62), (0.33, 0.63), and (0.33, 0.63), respectively. The tiny difference in the CIE coordinates might be ascribed to the distribution variation of the dopant in the emission layer (EML), which results in the diversity of the emission zone (EMZ).^[45]

In this study, two types of dispirocyclic compounds, namely dispiro[fluorene-9,9'-anthracene-10',9''-fluorene] (DSFA) and dispiro[acridine-9,9'-anthracene-10',9''-acridine] (DSAA), were used to construct host materials (**1**, **2**, **3**, and **4**) for green PHOLEDs. The preparation, characterization, and basic photophysical/electrochemical/EL properties of four new hosts were studied in detail. The variation in their molecular configuration has a profound effect on their basic physical, charge transport, and EL properties. The device based on **2** containing DSFA has the best device performance with a PE of over 100 lm W⁻¹ among the four OLEDs, G1-G4. In addition, the device hosted by **3** containing DSAA also showed a high PE of 96.1 lm W⁻¹. This study will pave the way for the developing of highly efficient host materials using these dispirocycles as molecular platforms.

Materials Synthesis

Compound 2'-bromodispiro[fluorene-9,9'-anthracene-10',9''-fluorene] (**2a**) was prepared according to the previous literature.^[41] Compounds 2'-(*tert*-butyl)dispiro[fluorene-9,9'-anthracene-10',9''-fluorene] (**1**), 2'-bromo-10,10''-diphenyl-10*H*,10''*H*-dispiro[acridine-9,9'-anthracene-10',9''-acridine] (**3a**), and 2'-(*tert*-butyl)-10,10''-diphenyl-10*H*,10''*H*-dispiro[acridine-9,9'-anthracene-10',9''-acridine] (**4**) were synthesized according to the reported procedure.^[38a,41]

Preparation of **1**, **3a**, and **4**

1, white solid. ¹H NMR (600 MHz, Methylene Chloride-*d*₂): δ = 7.96 (d, *J* = 7.7 Hz, 4H), 7.45 (t, *J* = 7.5 Hz, 4H), 7.31 (q, *J* = 7.4 Hz, 4H), 7.24 (t, *J* = 8.4 Hz, 4H), 6.84 (d, *J* = 8.5 Hz, 1H), 6.81 – 6.76 (m, 2H), 6.43 – 6.35 (m, 3H), 6.29 (d, *J* = 8.5 Hz, 1H), 0.89 (s, 9H) ppm. ¹³C NMR (151 MHz, Methylene Chloride-*d*₂): δ = 157.32 (d, *J* = 13.8 Hz), 149.28, 140.52, 136.90, 136.70, 135.87, 133.36, 128.69 (d, *J* = 13.3 Hz), 128.34 (d, *J* = 7.4 Hz), 127.86, 127.48 (d, *J* = 13.5 Hz), 126.62 (d, *J* = 3.9 Hz), 125.20 (d, *J* = 4.8 Hz), 124.10, 120.15 (d, *J* = 17.5 Hz), 58.11, 57.67,

33.88, 30.50 ppm. MALDI-TOF-MS: m/z : calcd for $C_{42}H_{32}$: 536.718, found: 536.564. Anal. Calcd for $C_{42}H_{32}$ (%): C 93.99, H 6.01; found: C 94.04, H 6.13.

3a, white solid. 1H NMR (400 MHz, Chloroform- d): δ = 7.81 (s, 1H), 7.79 – 7.74 (m, 4H), 7.65 – 7.57 (m, 4H), 7.54 (d, J = 7.7 Hz, 3H), 7.48 – 7.42 (m, 1H), 7.35 (d, J = 8.6 Hz, 1H), 7.15 (d, J = 8.6 Hz, 1H), 7.06 (td, J = 7.4, 1.8 Hz, 2H), 7.01 – 6.92 (m, 4H), 6.89 (d, J = 7.8 Hz, 4H), 6.74 (dt, J = 10.4, 7.5 Hz, 4H), 6.43 (dd, J = 15.5, 8.3 Hz, 4H) ppm. MALDI-TOF-MS: m/z : calcd for $C_{50}H_{33}BrN_2$: 741.732, found: 741.538. Anal. Calcd for $C_{50}H_{33}BrN_2$ (%): C 80.97, H 4.48, N 3.78; found: C 81.03, H 4.50, N 3.72.

4, white solid. 1H NMR (600 MHz, Chloroform- d): δ = 7.73 (t, J = 7.7 Hz, 4H), 7.62 – 7.54 (m, 6H), 7.53 – 7.49 (m, 2H), 7.48 (d, J = 2.2 Hz, 1H), 7.37 (d, J = 8.4 Hz, 1H), 7.08 – 6.99 (m, 3H), 6.95 – 6.87 (m, 8H), 6.74 – 6.63 (m, 4H), 6.43 – 6.36 (m, 4H), 1.12 (s, 9H) ppm. ^{13}C NMR (151 MHz, Chloroform- d): δ = 149.11, 143.44, 143.07, 142.65, 141.56, 141.37, 140.19 (d, J = 8.3 Hz), 139.81, 131.98 (d, J = 10.8 Hz), 131.76, 131.26 (d, J = 5.3 Hz), 131.00, 130.52, 130.18, 128.31 (d, J = 7.9 Hz), 127.39, 126.76 (d, J = 10.2 Hz), 126.46 (d, J = 11.2 Hz), 124.26, 120.44 (d, J = 5.7 Hz), 114.41 (d, J = 8.5 Hz), 49.22, 48.71, 34.26, 31.14 ppm. MALDI-TOF-MS: m/z : calcd for $C_{54}H_{42}N_2$: 718.944, found: 718.878. Anal. Calcd for $C_{54}H_{42}N_2$ (%): C 90.21, H 5.89, N 3.90; found: C 90.28, H 5.92, N 3.96.

Preparation of **2** and **3**

2a (2 g, 3.6 mmol), (4-(diphenylamino)phenyl)boronic acid (1.25 g, 4.3 mmol), potassium carbonate (K_2CO_3) (1 g, 7.2 mmol), and tetrakis(triphenylphosphine) palladium(0) ($Pd(PPh_3)_4$) (0.16 g, 0.14 mmol) were added into 1,4-dioxane (100 mL) under argon before the addition of water (10 mL). The resulting solution was heated at 95 °C overnight. After cooling down to room temperature, the product was extracted with dichloromethane for three times. The organic layer was collected, dried over (anhydrous sodium sulfate, Na_2SO_4), and evaporated. The crude product was subjected to column chromatography (petroleum ether/dichloromethane: 4/1, V/V) to obtain **2** as a white powder (yield: 2.3 g, 87%). 1H NMR (600 MHz, Methylene Chloride- d_2): δ = 7.98 (t, J = 8.1 Hz, 4H), 7.47 (dt, J = 10.0, 7.6 Hz, 4H), 7.34 (q, J = 7.2 Hz, 4H), 7.29 (d, J = 7.6 Hz, 4H), 7.20 (t, J = 8.7 Hz, 4H), 7.05 – 6.95 (m, 9H), 6.87 (d, J = 8.7 Hz, 2H), 6.82 – 6.80 (m, 2H), 6.55 (s, 1H), 6.44 (d, J = 8.5 Hz, 1H), 6.41 – 6.39 (m, 2H) ppm. ^{13}C NMR (151 MHz, Methylene Chloride- d_2): δ = 157.14 (d, J = 6.9 Hz), 147.48, 147.08, 140.56 (d, J = 2.8 Hz), 138.93, 136.93, 136.62, 136.46, 135.19, 133.92, 129.13, 128.68 (d, J = 5.8 Hz), 128.49 (d,

$J = 2.0$ Hz), 127.66 (d, $J = 4.6$ Hz), 127.23, 126.75 (d, $J = 2.8$ Hz), 126.39, 125.32, 125.13, 124.28, 123.44, 122.88, 120.32 (d, $J = 7.5$ Hz), 58.01, 57.76 ppm. MALDI-TOF-MS: m/z : calcd for $C_{56}H_{37}N$: 723.919, found: 723.878. Anal. Calcd for $C_{56}H_{37}N$ (%): C 92.91, H 5.15, N 1.93; found: C 93.06, H 5.23, N 2.04.

Compound **3** was prepared with similar method as that for **2**. 1H NMR (600 MHz, Methylene Chloride- d_2): $\delta = 7.82$ (s, 1H), 7.79 (t, $J = 7.6$ Hz, 2H), 7.72 (t, $J = 7.6$ Hz, 2H), 7.64 (dd, $J = 16.5, 7.8$ Hz, 2H), 7.59 (d, $J = 7.7$ Hz, 2H), 7.56 (d, $J = 7.4$ Hz, 3H), 7.51 (t, $J = 9.0$ Hz, 2H), 7.32 (d, $J = 8.4$ Hz, 1H), 7.29 – 7.23 (m, 6H), 7.15 – 7.08 (m, 6H), 7.06 – 7.03 (m, 4H), 7.00 – 6.90 (m, 8H), 6.75 (q, $J = 6.9$ Hz, 4H), 6.44 (d, $J = 8.3$ Hz, 4H) ppm. ^{13}C NMR (151 MHz, Methylene Chloride- d_2): $\delta = 147.60, 147.25, 143.86$ (d, $J = 9.1$ Hz), 142.18, 141.16, 140.94, 140.82, 140.18, 140.05, 139.13, 134.46, 131.72, 131.61, 131.50, 131.45, 131.38, 131.15 (d, $J = 9.3$ Hz), 131.01, 130.33, 129.17, 128.55 (d, $J = 6.8$ Hz), 128.23, 127.56, 127.11, 126.92, 126.68, 125.36, 124.31, 123.66, 122.90, 120.56 (d, $J = 6.8$ Hz), 114.73, 49.03, 48.64 ppm. MALDI-TOF-MS: m/z : calcd for $C_{68}H_{47}N_3$: 906.145, found: 906.124. Anal. Calcd for $C_{68}H_{47}N_3$ (%): C 90.13, H 5.23, N 4.64; found: C 90.19, H 5.28, N 4.52.

Experimental

Measurements and Characterization

All chemicals and reagents were used as received from commercial sources without further purification. THF was purified by PURE SOLV (Innovative Technology) purification system. 1H NMR and ^{13}C NMR spectra were recorded in chloroform- d ($CDCl_3$) on a Bruker 400 and Agilent DD2-600 MHz NMR spectrometer at room temperature. Matrix-Assisted Laser Desorption/ Ionization Time of Flight Mass Spectrometry (MALDI-TOF-MS) was measured with a BRUKER ultrafleXtreme MALDI-TOF/TOF. UV-vis absorption spectra were recorded on Cary 60 spectrometer (Agilent Technologies). PL spectra and phosphorescent spectra were recorded on a Hitachi F-4600 fluorescence spectrophotometer. Differential scanning calorimetry (DSC) was performed on a TA DSC 2010 unit at a heating rate of $10\text{ }^\circ\text{C min}^{-1}$ under nitrogen. The glass transition temperatures (T_g) were determined from the second heating scan. Thermogravimetric analysis (TGA) was performed on a TA SDT 2960 instrument at a heating rate of $10\text{ }^\circ\text{C min}^{-1}$ under nitrogen. Temperature at 5% weight loss was used as the decomposition temperature (T_d). Cyclic voltammetry (CV) was carried out on a CHI600 voltammetric analyzer at room temperature with ferrocenium-ferrocene (Fc^+/Fc) as the internal standard. The oxidative scans were performed using 0.1 M $n\text{-Bu}_4\text{NPF}_6$ (TBAPF₆) in deaerated

DMF as the supporting electrolyte. A conventional three-electrode configuration consisting of a Pt-wire counter electrode, an Ag/AgCl reference electrode, and a platinum working electrode was used. The cyclic voltammograms were measured at a scan rate of 100 mV s⁻¹. DFT calculations were performed using B3LYP/6-31 G(d) basis set using Gaussian 09.

Device fabrication and characterization

The OLEDs were fabricated on the indium-tin oxide (ITO) coated transparent glass substrates, the ITO conductive layer having a thickness of ca. 100 nm and a sheet resistance of ca. 30 Ω per-square. The active area of each device is 0.09 cm². The ITO glasses were ultrasonically cleaned by ethanol, acetone and deionized water for 10 min subsequently, and then exposed to UV-ozone for 15 min. All of the organic materials and metal layers under a vacuum of ca. 10⁻⁶ Torr. The deposition rate was controlled at 2 Å s⁻¹ for HAT-CN, 0.2-0.4 Å s⁻¹ for Liq, 1-2 Å s⁻¹ for other organic layers and 5-8 Å s⁻¹ for Al anode. The EL spectra, CIE coordinates, *J-V-L* curves, CE, and PE of the devices were measured with a programmable spectra scan photometer (PHOTO RESEARCH, PR 655) and a constant current source meter (KEITHLEY 2400) at room temperature.

Supporting Information

Supporting Information is available from the Wiley Online Library or from the author.

Acknowledgements

We acknowledge financial support from the National Key R&D Program of China (2016YFB0400703), the National Natural Science Foundation of China (21472135, 61307036), Natural Science Foundation of Jiangsu Province of China (BK20151216), and the 111 Project. This project is also funded by Collaborative Innovation Center of Suzhou Nano Science and Technology (CIC-Nano), Joint International Research Laboratory of Carbon-Based Functional Materials and Devices, Soochow University and by the Priority Academic Program Development of Jiangsu Higher Education Institutions (PAPD).

Received: ((will be filled in by the editorial staff))

Revised: ((will be filled in by the editorial staff))

Published online: ((will be filled in by the editorial staff))

[1] R. G. Clarkson, M. Gomberg, *J. Am. Chem. Soc.* **1930**, 52, 2881.

- [2] (a) C. Poriel, Y. Ferrand, P. le Maux, C. Paul, J. Rault-Berthelot, G. Simonneaux, *Chem. Commun.* **2003**, 18, 2308; (b) C. Poriel, A. Martail, G. Simonneaux, *Inorg. Chem. Commun.* **2007**, 10, 627.
- [3] (a) D. K. Smith, A. Zingg, F. Diederich, *Helv. Chim. Acta* **1999**, 82, 1225; (b) G. Das, A. D. Hamilton, *Tetrahedron Lett.* **1997**, 38, 3675; (c) A. Tejada, A. I. Oliva, L. Simon, M. Grande, M. C. Caballero, J. R. Moran, *Tetrahedron Lett.* **2000**, 41, 4563.
- [4] (a) J. H. Fournier, T. Maris, J. D. Wuest, *J. Org. Chem.* **2004**, 69, 1762; (b) E. Demers, T. Maris, J. D. Wuest, *Cryst. Growth Des.* **2005**, 5, 1227; (c) K. T. Wong, Y. L. Liao, Y. C. Peng, C. C. Wang, S. Y. Lin, C. H. Yang, S. M. Tseng, G. H. Lee, S. M. Peng, *Cryst. Growth Des.* **2005**, 5, 667; (d) F. Moreau, N. Audebrand, C. Poriel, V. Moizan-Baslé, J. Ouvry, *J. Mater. Chem.* **2011**, 21, 18715.
- [5] (a) J. Weber, A. Thomas, *J. Am. Chem. Soc.* **2008**, 130, 6334; (b) J. Schmidt, M. Werner, A. Thomas, *Macromolecules* **2009**, 42, 4426; (c) S. Thomas, I. Pinnau, N. Y. Du, M. D. Guiver, *J. Membr. Sci.* **2009**, 333, 125.
- [6] C. L. Chiang, S. M. Tseng, C. T. Chen, C. P. Hsu, C. F. Shu, *Adv. Funct. Mater.* **2008**, 18, 248.
- [7] A. Aviram, *J. Am. Chem. Soc.* **1988**, 110, 5687.
- [8] (a) J. M. Tour, R. Wu, J. S. Schumm, *J. Am. Chem. Soc.* **1990**, 112, 5662; (b) J. M. Tour, R. Wu, J. S. Schumm, *J. Am. Chem. Soc.* **1991**, 113, 7064.
- [9] J. Salbeck, N. Yu, J. Bauer, F. Weissörtel, H. Bestgen, *Synth. Met.* **1997**, 91, 209.
- [10] U. Bach, D. Lupo, P. Comte, J. E. Moser, F. Weissortel, J. Salbeck, H. Spreitzer, M. Gratzel, *Nature* **1998**, 395, 583.
- [11] D. Shi, X. Qin, Y. Li, Y. He, C. Zhong, J. Pan, H. Dong, W. Xu, T. Li, W. Hu, J.-L. Brédas, O. M. Bakr, *Sci. Adv.* **2016**, 2, e1501491.
- [12] W. L. Yu, J. Pei, W. Huang, A. J. Heeger, *Adv. Mater.* **2000**, 12, 828.
- [13] (a) J. Pei, J. Ni, X.-H. Zhou, X.-Y. Cao, Y.-H. Lai, *J. Org. Chem.* **2002**, 67, 4924; (b) X. Zhang, J.-B. Han, P. F. Li, X. Ji, Z. Zhang, *Synth. Commun.* **2009**, 39, 3804.
- [14] (a) L.-S. Cui, S.-C. Dong, Y. Liu, M.-F. Xu, Q. Li, Z.-Q. Jiang, L.-S. Liao, *Org. Electron.* **2013**, 14, 1924; (b) L.-S. Cui, Y.-M. Xie, Y.-K. Wang, C. Zhong, Y.-L. Deng, X.-Y. Liu, Z.-Q. Jiang, L.-S. Liao, *Adv. Mater.* **2015**, 27, 4213; (c) L.-S. Cui, S.-B. Ruan, F. Bencheikh, R. Nagata, L. Zhang, K. Inada, H. Nakanotani, L.-S. Liao, C. Adachi, *Nat. Commun.* **2017**, 8, 2250.
- [15] (a) C. Poriel, J. Rault-Berthelot, *J. Mater. Chem. C* **2017**, 5, 3869; (b) Z. Jiang, H. Yao, Z. Zhang, C. Yang, Z. Liu, Y. Tao, J. Qin, D. Ma, *Org. Lett.* **2009**, 11, 2607.

- [16] L. Sicard, C. Quinton, J.-D. Peltier, D. Tondelier, B. Geffroy, U. Biapo, R. Métivier, O. Jeannin, J. Rault-Berthelot, C. Poriel, *Chem. Eur. J.* **2017**, *23*, 7719.
- [17] (a) W.-F. Jiang, H.-L. Wang, A.-G. Wang, Z. Q. Li, *Synth. Commun.* **2008**, *38*, 1888; (b) W. Y. Huang, S. Y. Huang, *Macromolecules* **2010**, *43*, 10355; (c) K. Esashika, M. Yoshizawa-Fujita, Y. Takeoka, M. Rikukawa, *Synth. Met.* **2009**, *159*, 2184.
- [18] (a) L. Wang, B. Pan, L. Zhu, B. Wang, Y. Wang, Y. Liu, J. Jin, J. Chen, D. Ma, *Dyes Pigments* **2015**, *114*, 222; (b) Y. Mo, X. Jiang, D. Cao, *Org Lett.* **2007**, *9*, 4371; (c) X. Zhang, C. Jiang, Y. Mo, Y. Xu, H. Shi, Y. Cao, *Appl. Phys. Lett.* **2006**, *88*, 051116; (d) Y. Mo, L. Du, L. Liu, J. Huang, Y. Pan, B. Yang, Z. Xie, Y. Ma, *J. Phys. Chem. C* **2013**, *117*, 27081.
- [19] (a) V. Prelog, *Pure Appl. Chem.* **1978**, *50*, 893; (b) V. Prelog, D. Bedeković, *Helv. Chim. Acta* **1979**, *62*, 2285; (c) F. Thiemann, T. Piehler, D. Haase, W. Saak, A. Lutzen, *Eur. J. Org. Chem.* **2005**, 1991; (d) X. Cheng, G. H. Hou, J. H. Xie, Q. L. Zhou, *Org. Lett.* **2004**, *6*, 2381; (e) X. Cheng, S. F. Zhu, X. C. Qiao, P. C. Yan, Q. L. Zhou, *Tetrahedron* **2006**, *62*, 8077.
- [20] (a) D. Curiel, M. Más-Montoya, G. Sánchez, *Coord. Chem. Rev.* **2015**, *284*, 19; (b) R. Hovorka, S. Hytteballe, T. Piehler, G. Meyer-Eppler, F. Topić, K. Rissanen, M. Engeser, A. Lützen, *Beilstein J. Org. Chem.* **2014**, *10*, 432; (c) R. Hovorka, G. Meyer-Eppler, T. Piehler, S. Hytteballe, M. Engeser, F. Topić, K. Rissanen, A. Lützen, *Chem. Eur. J.* **2014**, *20*, 13253; (d) J. Dong, Y. Liu, Y. Cui, *Chem. Commun.* **2014**, *50*, 14949; (e) Q. Fang, S. Gu, J. Zheng, Z. Zhuang, S. Qiu, Y. Yan, *Angew. Chem. Int. Ed.* **2014**, *53*, 2878; (f) W. Yao, Q. Liu, Y. Shi, J. Tang, *Heterocycles* **2012**, *85*, 1077.
- [21] (a) Z. Wu, B. Han, C. Zhang, D. Zhu, L. Gao, M. Ding, Z. Yang, *Polymer* **2012**, *53*, 5706; (c) X. Cheng, Q. Zhang, J.-H. Xie, L.-X. Wang, Q.-L. Zhou, *Angew. Chem. Int. Ed.* **2005**, *44*, 1118; (d) C.-L. Chiang, C.-F. Shu, C.-T. Chen, *Org. Lett.* **2005**, *17*, 3717.
- [22] (a) D. Hellwinkel, G. Haas, *Liebigs Ann. Chem.* **1978**, *1978*, 1913; (b) H. Oyama, M. Akiyama, K. Nakano, M. Naito, K. Nobusawa, K. Nozaki, *Org. Lett.* **2016**, *18*, 3654; (c) Y. Liu, Y. L. S. Tse, F. Y. Kwong, Y. Y. Yeung, *ACS Catal.* **2017**, *7*, 4453; (d) S. F. Gait, M. E. Peek, C. W. Rees, R. C. Storr, *J. Chem. Soc., Perkin Trans.* **1974**, *1*, 1248.
- [23] (a) E. H. Huntress, I. S. Cliff, *J. Am. Chem. Soc.* **1933**, *55*, 2559; (b) S. Kajigaeshi, K. Kobayashi, S. Kurata, A. Kitajima, F. Nakahara, H. Nago, A. Nishiida, S. Fujisaki, *Nippon Kagaku Kaishi* **1989**, *12*, 2052; (c) X.-Y. Chen, S. Ozturk, E. J. Sorensen, *Org. Lett.* **2017**, *19*, 1140.
- [24] (a) L.-H. Xie, J. Liang, J. Song, C.-R. Yin, W. Huang, *Curr. Org. Chem.* **2010**, *14*, 2169; (b) R. Pudzich, T. Fuhrmann-Lieker, J. Salbeck, *Adv. Polym. Sci.* **2006**, *199*, 83.

- [25] (a) D. M. Bassani, L. Jonusauskaite, A. Lavie-Cambot, N. D. McClenaghan, J.-L. Pozzo, D. Ray, G. Vives, *Coord. Chem. Rev.* **2010**, *254*, 2429; (b) H. Haick, D. Cahen, *Prog. Surf. Sci.* **2008**, *83*, 217; (c) M. Valášek, K. Edelmann, L. Gerhard, O. Fuhr, M. Lukas, M. Mayor, *J. Org. Chem.* **2014**, *79*, 7342; (d) N. J. Jeon, H. G. Lee, Y. C. Kim, J. Seo, J. H. Noh, J. Lee, S. I. Seok, *J. Am. Chem. Soc.* **2014**, *136*, 7837; (e) K.-T. Wong, Y.-L. Liao, Y.-T. Lin, H.-C. Su, C.-C. Wu, *Org. Lett.* **2005**, *23*, 5131; (f) M.-Y. Lai, C.-H. Chen, W.-S. Huang, J. T. Lin, T.-H. Ke, L.-Y. Chen, M.-H. Tsai, C.-C. Wu, *Angew. Chem. Int. Ed.* **2008**, *47*, 581; (g) Y. Lin, Z.-K. Chen, T.-L. Ye, Y.-F. Dai, D.-G. Ma, Z. Ma, Q.-D. Liu, Y. Chen, *Polymer* **2010**, *51*, 1270; (h) G. Liaptsis, D. Hertel, K. Meerholz, *Angew. Chem. Int. Ed.* **2013**, *52*, 9563.
- [26] (a) R. Wu, J. S. Schumm, D. L. Pearson, J. M. Tour, *J. Org. Chem.* **1996**, *61*, 6906; (b) Y. Lin, Z.-K. Chen, T.-L. Ye, Y.-F. Dai, D.-G. Ma, Z. Ma, Q.-D. Liu, Y. Chen, *J. Polym. Sci. A Polym. Chem.* **2010**, *48*, 292; (c) R. Seto, T. Sato, T. Kojima, K. Hosokawa, Y. Koyama, G.-I. Konishi, T. Takata, *J. Polym. Sci. A Polym. Chem.* **2010**, *48*, 3658.
- [27] (a) S. Tang, M. Liu, C. Gu, Y. Zhao, P. Lu, D. Lu, L. Liu, F. Shen, B. Yang, Y. Ma, *J. Org. Chem.* **2008**, *73*, 4212; (b) Y. Wu, J. Zhang, Z. Bo, *Org. Lett.* **2007**, *9*, 4435.
- [28] L. Pop, F. Dumitru, N. D. Hädade, Y.-M. Legrand, A. van der Lee, M. Barboiu, I. Grosu, *Org. Lett.* **2015**, *17*, 3494.
- [29] (a) T. P. I. Saragi, T. Spehr, A. Siebert, T. Fuhrmann-Lieker, J. Salbeck, *Chem. Rev.* **2007**, *107*, 1011; (b) R. Pudzich, T. Fuhrmann-Lieker, J. Salbeck, *Adv. Polym. Sci.* **2006**, *199*, 83.
- [30] (a) W.-C. Chen, Y. Yuan, Z.-L. Zhu, S.-F. Ni, Z.-Q. Jiang, L.-S. Liao, F.-L. Wong, C.-S. Lee, *Chem. Commun.* **2018**, *54*, 4541; (b) M.-M. Xue, C.-C. Huang, Y. Yuan, L.-S. Cui, Y.-X. Li, B. Wang, Z.-Q. Jiang, M.-K. Fung, L.-S. Liao, *ACS Appl. Mater. Interfaces* **2016**, *8*, 20230.
- [31] (a) C.-J. Lin, H.-L. Huang, M.-R. Tseng, C.-H. Cheng, *J. Disp. Technol.* **2009**, *5*, 236; (b) K. Nasu, T. Nakagawa, H. Nomura, C.-J. Lin, C.-H. Cheng, M.-R. Tseng, T. Yasuda, C. Adachi, *Chem. Commun.* **2013**, *49*, 10385.
- [32] (a) M. Romain, D. Tondelier, B. Geffroy, A. Shirinskaya, O. Jeannin, J. Rault-Berthelot, C. Poriel, *Chem. Commun.* **2015**, *51*, 1313; (b) M. Romain, D. Tondelier, O. Jeannin, B. Geffroy, J. Rault-Berthelot, C. Poriel, *J. Mater. Chem. C* **2015**, *3*, 9701; (c) W. Zhang, J. Jin, Z. Huang, S. Zhuang, L. Wang, *Sci. Rep.* **2016**, *6*, 30178.
- [33] (a) M. Liu, R. Komatsu, X. Cai, K. Hotta, S. Sato, K. Liu, D. Chen, Y. Kato, H. Sasabe, S. Ohisa, Y. Suzuri, D. Yokoyama, S.-J. Su, J. Kido, *Chem. Mater.* **2017**, *29*, 8630; (b) N. A.

WILEY-VCH

- Drigo, L. G. Kudriashova, S. Weissenseel, A. Sperlich, A. J. Huckaba, M. K. Nazeeruddin, V. Dyakonov, *J. Phys. Chem. C* **2018**, *122*, 22796.
- [34] X.-Y. Liu, X. Tang, Y. Zhao, D. Zhao, J. Fan, L.-S. Liao, *J. Mater. Chem. C* **2018**, *6*, 1023.
- [35] G. Tian, W. Liang, Y. Chen, N. Xiang, Q. Dong, J. Huang, J.-H. Su, *Dyes Pigments* **2016**, *126*, 296.
- [36] (a) C. Poriel, J.-J. Liang, J. Rault-Berthelot, F. Barrière, N. Cocherel, A. M. Z. Slawin, D. Horhant, M. Virboul, G. Alcaraz, N. Audebrand, L. Vignau, N. Huby, G. Wantz, L. Hirsch, *Chem. Eur. J.* **2007**, *13*, 10055; (b) M. Romain, D. Tondelier, J.-C. Vanel, B. Geffroy, O. Jeannin, J. Rault-Berthelot, R. Métivier, C. Poriel, *Angew. Chem. Int. Ed.* **2013**, *52*, 14147; (c) M. Romain, S. Thiery, A. Shirinskaya, C. Declairieux, D. Tondelier, B. Geffroy, O. Jeannin, J. Rault-Berthelot, R. Métivier, C. Poriel, *Angew. Chem. Int. Ed.* **2015**, *54*, 1176; (d) D. Thirion, M. Romain, J. Rault-Berthelot, C. Poriel, *J. Mater. Chem.* **2012**, *22*, 7149; (e) M. Romain, D. Tondelier, B. Geffroy, O. Jeannin, E. Jacques, J. Rault-Berthelot, C. Poriel, *Chem. Eur. J.* **2015**, *21*, 9426; (f) C. Poriel, J. Rault-Berthelot, *Acc. Chem. Res.* **2018**, *51*, 1818.
- [37] Y.-J. Cho, O.-Y. Kim, J.-Y. Lee, *Org. Electron.* **2012**, *13*, 351.
- [38] (a) B. Li, Y. Qiu, L. Wang, Y. Gao, *Jpn. J. Appl. Phys.* **2002**, *41*, 5599; (b) K. H. Lee, S. O. Kim, K. S. Yook, S. O. Jeon, J. Y. Lee, S. S. Yoon, *Synth. Met.* **2011**, *161*, 2024; (c) K. H. Lee, S. O. Kim, J. N. You, S. Kang, J. Y. Lee, K. S. Yook, S. O. Jeon, J. Y. Lee, S. S. Yoon, *J. Mater. Chem.* **2012**, *22*, 5145.
- [39] X.-Y. Liu, X. Tang, Y. Zhao, D. Zhao, J. Fan, L.-S. Liao, *ACS Appl. Mater. Interfaces* **2018**, *10*, 1925.
- [40] (a) B. Li, Y. Qiu, F. Wang, CN 1338499, **2002**; (b) J. S. Ha, S. G. Hong, W. P. Hong, KR 2017041648 A, **2017**.
- [41] K.-K. Kim, S. Son, S. Yoon, J.-S. Bae, Y.-G. Lee, S.-G. Im, J. Kim, J.-C. Lee, US Pat. 6,984,462, **2006**.
- [42] (a) Z. Chen, Z. Wu, F. Ni, C. Zhong, W. Zeng, D. Wei, K. An, D. Ma, C. Yang, *J. Mater. Chem. C* **2018**, *6*, 6543; (b) C. Li, X. Fan, C. Han, H. Xu, *J. Mater. Chem. C* **2018**, *6*, 6747.
- [43] (a) Y. Tao, Q. Wang, C. Yang, C. Zhong, J. Qin, D. Ma, *Adv. Funct. Mater.* **2010**, *20*, 2923; (b) M. G. Helander, Z. B. Wang, J. Qiu, M. T. Greiner, D. P. Puzzo, Z. W. Liu, Z. H. Lu, *Science* **2011**, *332*, 944; (c) J. Liang, C. Li, X. Zhuang, K. Ye, Y. Liu, Y. Wang, *Adv. Funct. Mater.* **2018**, *28*, 1707002.
- [44] J. Zhao, G.-H. Xie, C.-R. Yin, L.-H. Xie, C.-M. Han, R.-F. Chen, H. Xu, M.-D. Yi, Z.-P.

WILEY-VCH

Deng, S.-F. Chen, Y. Zhao, S.-Y. Liu, W. Huang, *Chem. Mater.* **2011**, *23*, 5331.

[45] G. Liaptsis, K. Meerholz, *Adv. Funct. Mater.* **2013**, *23*, 359.

Accepted Manuscript

WILEY-VCH

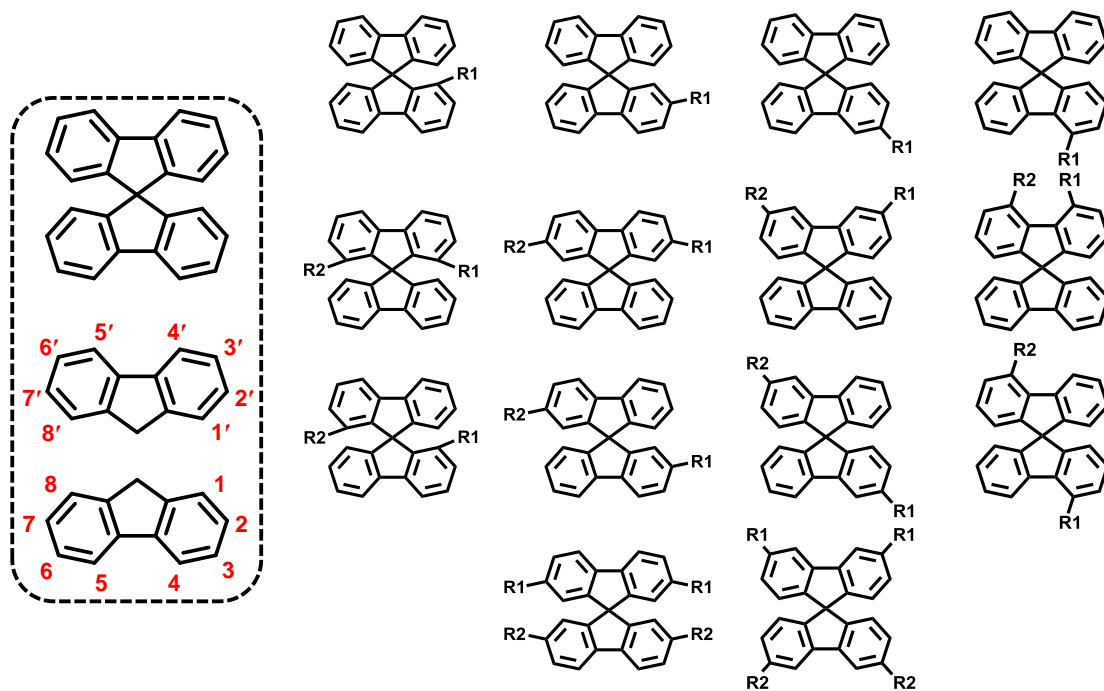


Figure 1. General formula for mono-, di-, and tetra-substituted SBF derivatives.

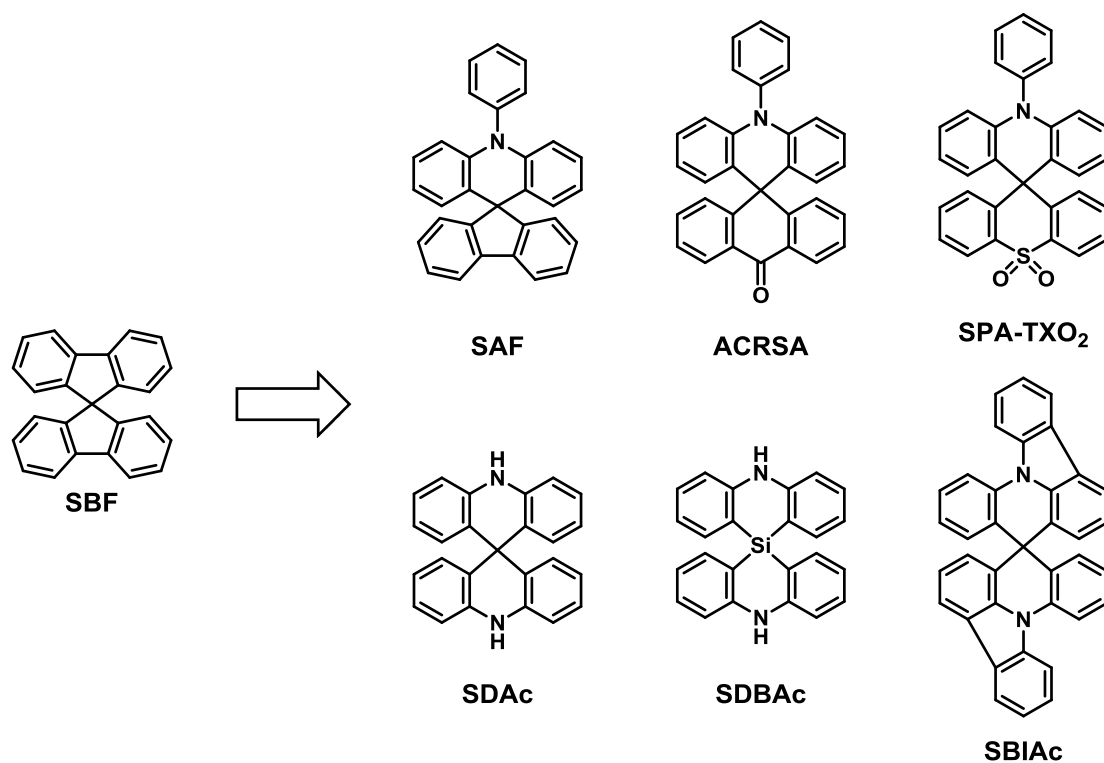


Figure 2. Molecule structures of SBF analogues.

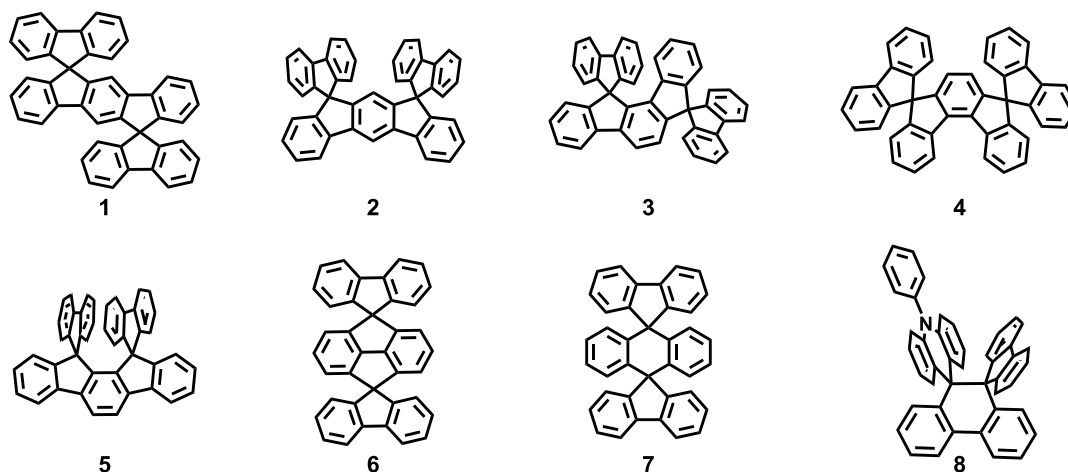
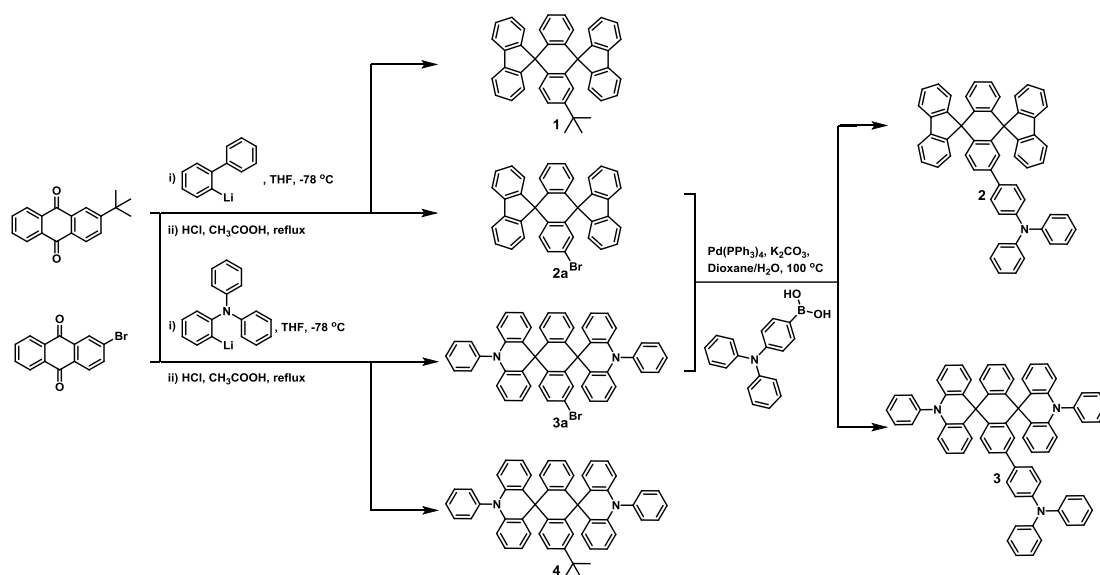


Figure 3. Representative dispiro-type OLED materials.



Scheme 1 Molecular structure and synthetic routes of 1, 2, 3, and 4.

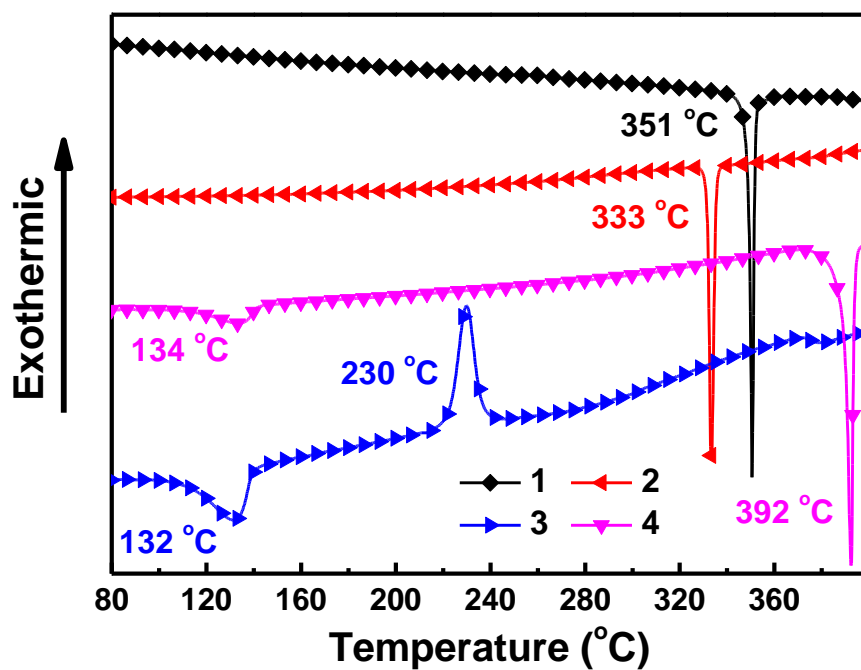


Figure 4. DSC curves of 1, 2, 3, and 4.

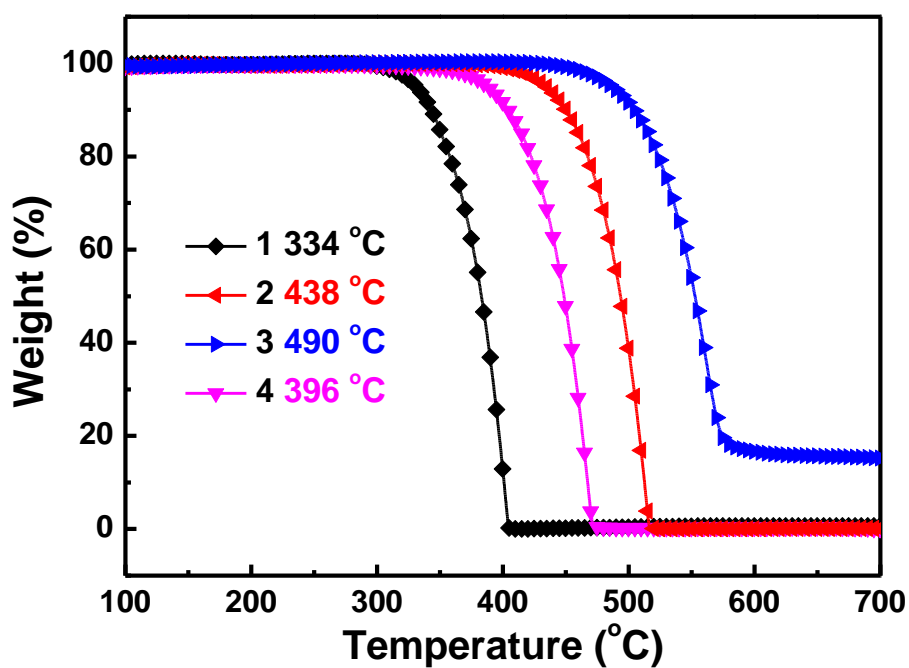


Figure 5. TGA curves of 1, 2, 3, and 4.

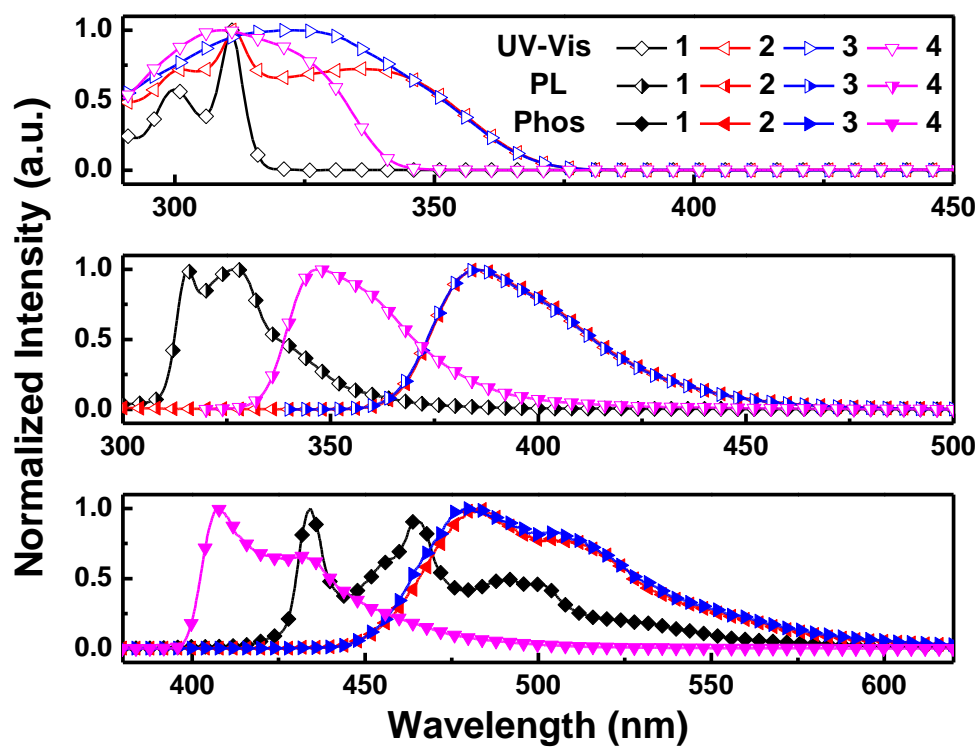


Figure 6. UV-Vis absorption, PL, and Phos spectra of **1**, **2**, **3**, and **4** in toluene solution.

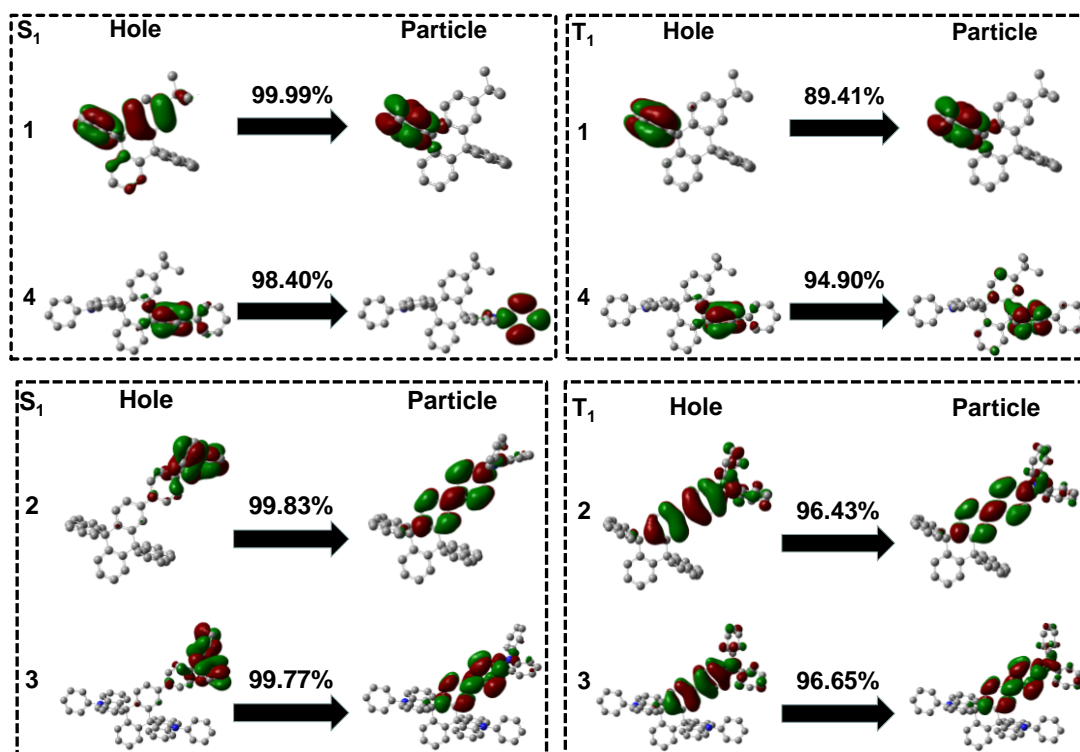


Figure 7. The natural transition orbital (NTO) analysis of 1, 2, 3, and 4.

WILEY-VCH

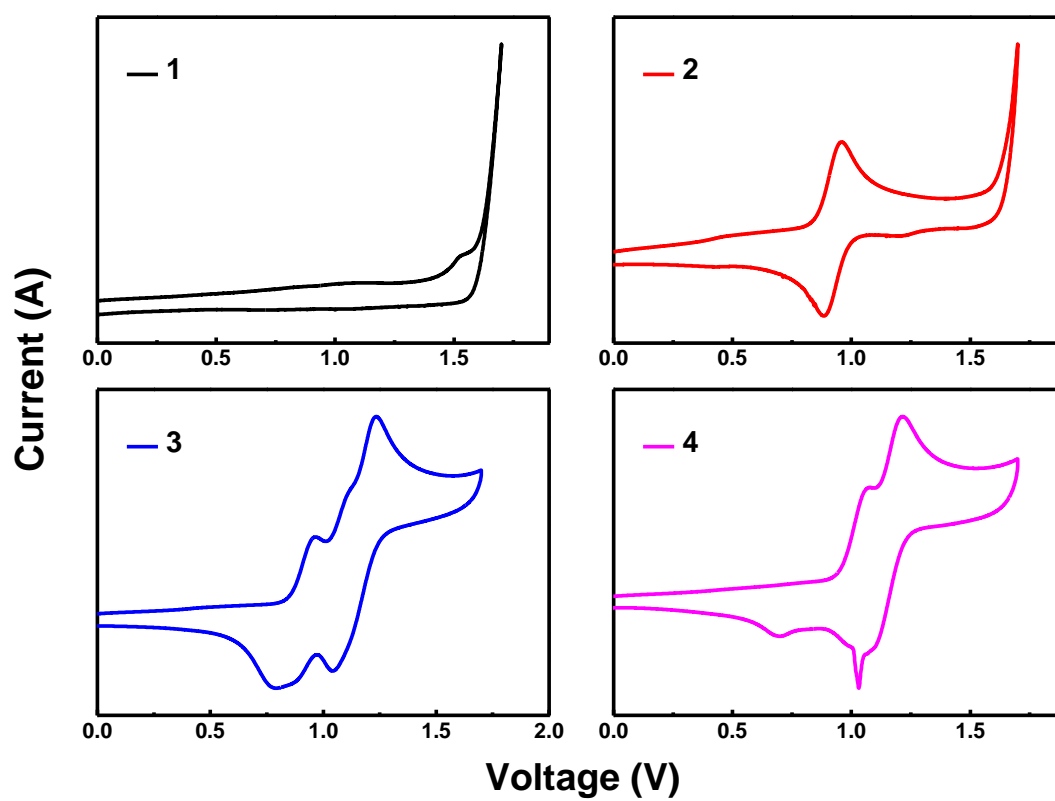


Figure 8. Cyclic voltammograms of 1, 2, 3, and 4.

Accepted Manuscript

WILEY-VCH

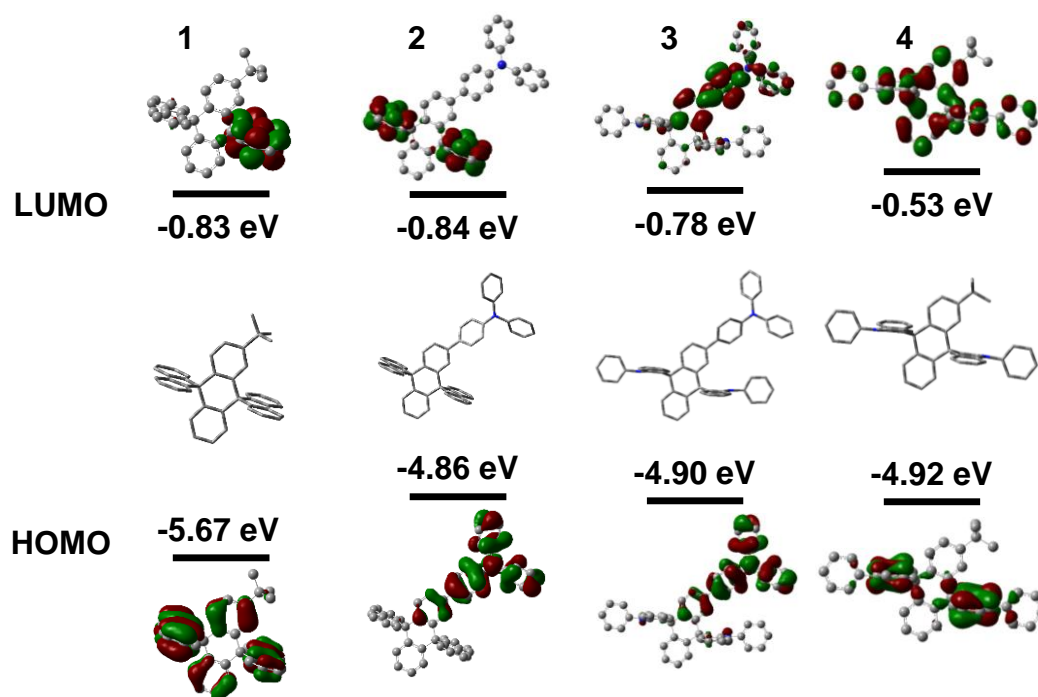


Figure 9. HOMO/LUMO distributions and energy levels and optimized geometry of **1**, **2**, **3**, and **4**.

Table 1. Physical properties of **1**, **2**, **3**, and **4**.

Host	Abs $\lambda_{\max}^{\text{a)}$ [nm]	PL $\lambda_{\max}^{\text{a)}$ [nm]	$T_{\text{g}}^{\text{b)}}$ / $T_{\text{c}}^{\text{c)}}$ / $T_{\text{m}}^{\text{d)}}$ / $T_{\text{d}}^{\text{e)}$ [°C]	$E_{\text{g}}^{\text{f)}$ [eV]	$E_{\text{T}}^{\text{g)}$ [eV]	HOMO ^{h)} [eV]	LUMO ⁱ⁾ [eV]
1	300, 311	316, 327	-/-/351/334	3.92	2.86	-5.82	-1.90
2	300, 311, 337	385	-/-/333/438	3.35	2.57	-5.23	-1.88
3	323	385	132/230/-/490	3.35	2.58	-5.24	-1.89
4	310	348	134/-/392/396	3.63	3.04	-5.34	-1.71

a) Measured in toluene solution at room temperature.

b) T_{g} : Glass transition temperature.

c) T_{c} : Crystallization temperature.

d) T_{m} : Melting point.

e) T_{d} : Decomposition temperature.

f) E_{g} : Band gap energies were calculated from the corresponding absorption onsets.

g) E_{T} : Measured in toluene glass matrix at 77 K.

h) HOMO levels were calculated from CV data.

i) LUMO levels were calculated from the HOMOs and E_{gs} .

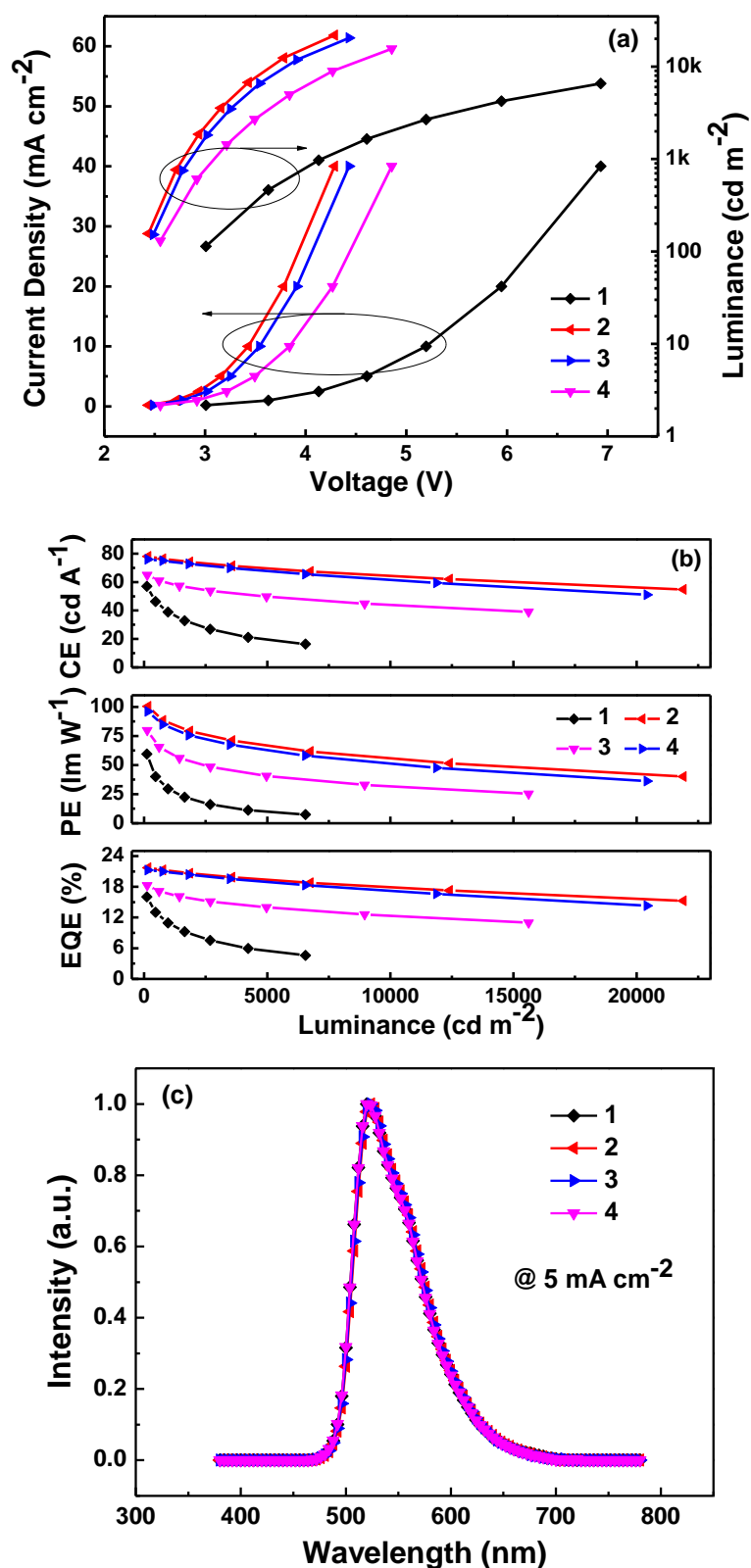


Figure 10. (a) J - V - L characteristics, (b) CE-, PE-, and EQE- L curves, and (c) EL spectra of green devices.

WILEY-VCH

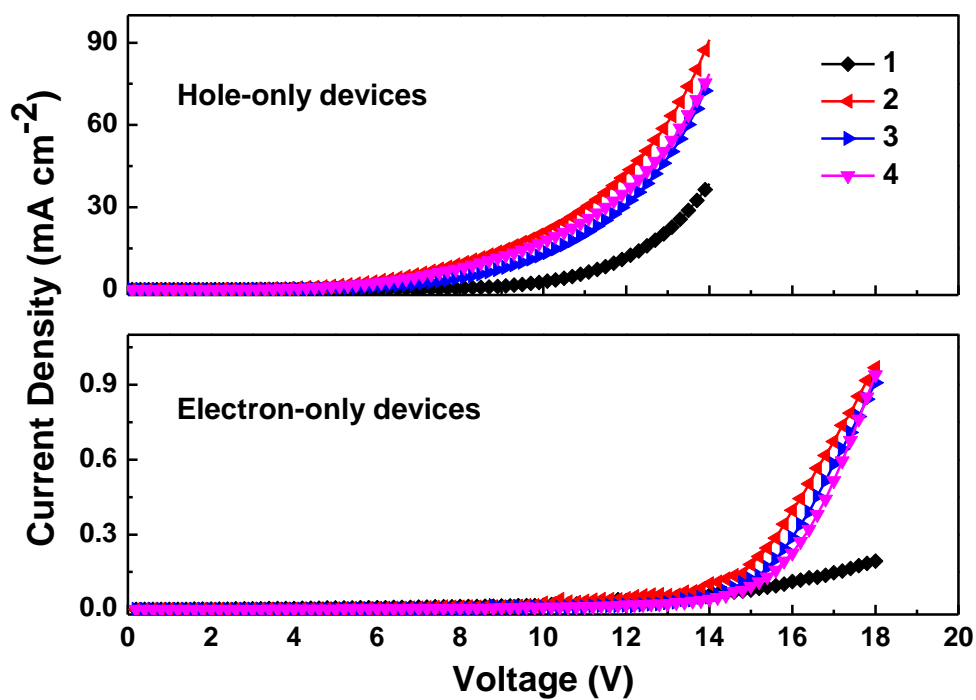


Figure 11. J - V characteristics curves of single carrier devices.

Accepted Manuscript

Table 2. Electroluminescence characteristics of the green and red devices.

Device ^a	Host ^a	V^b	η_{CE}^c	η_{PE}^c	EQE ^c	CIE ^d
		[V]	[cd A ⁻¹]	[lm W ⁻¹]	[%]	[x, y]
G1	1	3.24	57.0, 46.2	59.5, 39.4	16.0, 13.2	0.33, 0.63
G2	2	2.47	78.0, 77.1	100.5, 93.4	21.7, 21.3	0.34, 0.62
G3	3	2.53	76.0, 75.5	96.1, 89.5	21.3, 21.0	0.33, 0.63
G4	4	2.65	65.0, 61.9	80.0, 69.2	18.3, 17.4	0.33, 0.63

a) The notation 1-4 in devices G1-G4 indicates the corresponding devices fabricated with **1**, **2**, **3**, and **4** as the host respectively. Device configuration: G1-G4: ITO/ HAT-CN (10 nm)/ TAPC (55 nm)/ Host: 10 wt% Ir(ppy)₂(acac) (20 nm)/ B4PyMPM (40 nm)/ Liq (2 nm)/ Al (120 nm).

b) Voltages at 200 cd m⁻².

c) Efficiencies in the order of the maxima and at 500 cd m⁻².

d) Commission International de l'Eclairage coordinates measured at 5 mA cm⁻².

WILEY-VCH

The table of contents entry: Dispirocycles molecular platforms as rigid building blocks to construct efficient host materials for phosphorescent organic light-emitting diodes

Keyword: Dispirocycles, Host materials, Phosphorescence, OLEDs, Triplet energy

Xiang-Yang Liu,[†] Yi-Jie Zhang,[†] Xiyu Fei, Man-Keung Fung,^{*} and Jian Fan^{*}

Dispirocycles: Novel Platforms for Construction of High-Performance Host Materials for Phosphorescent Organic Light-Emitting Diodes

